Available online at www.sciencedirect.com
ScienceDirect
International Journal of Mass Spectrometry 266 (2007) 86–91
International Journal of Mass Spectrometry
www.elsevier.com/locate/ijms

Gas-phase ion chemistry of NF_3/SO_2 mixtures: A mass spectrometric and theoretical investigation

Paola Antoniotti [a], Roberto Rabezzana [a], Francesca Turco [a], Stefano Borocci [b], Nicoletta Bronzolino [b], Felice Grandinetti [b,*]

[a] *Dipartimento di Chimica Generale ed Organica Applicata, Università di Torino, C.so Massimo d' Azeglio, 48, 10125 Torino, Italy*
[b] *Dipartimento di Scienze Ambientali, Università della Tuscia, L.go dell' Università, 01100 Viterbo, Italy*

Received 5 June 2007; received in revised form 18 July 2007; accepted 18 July 2007
Available online 25 July 2007

Abstract

The gas-phase ion chemistry of NF_3/SO_2 mixtures has been investigated by ion trap mass spectrometry and theoretical calculations. SO^+ and SO_2^+ react efficiently with NF_3 giving $F{-}(SO)^+$ and $F{-}(SO_2)^+$. CAD experiments and thermochemical considerations support the exclusive formation of the sulfur–fluorine cations $F{-}SO^+$ and $F{-}SO_2^+$. NF_2^+ is unreactive toward SO_2, and NF_3^+ undergoes exclusively the efficient charge transfer. On the other hand, NF^+ activates the $OS{-}O$ bond, with formation of SO^+ and NO^+. DFT and coupled cluster calculations indicate that these ionic products arise from a SO^+–(FNO) ion–dipole complex, which dissociates into SO^+ and FNO or NO^+ and FSO. This intermediate is more stable than NF^+ and SO_2 by nearly 60 kcal mol^{-1}. We have also located a less stable sulfur–nitrogen complex $FN{-}SO_2^+$, whose formation explains the less efficient observed charge transfer between NF^+ and SO_2. The only observed negative ion–molecule reaction is the formation of $F{-}SO_2^-$ from the reaction between SO_2^- and NF_3. Our investigated processes may be of interest for the plasma and the atmospheric chemistry of NF_3, one of the gaseous compounds most extensively used in the electronic industry to perform etching and cleaning processes.

Keywords: Ion trap mass spectrometry; Nitrogen trifluoride; Sulfur dioxide; Sulfur oxyfluorine ion; Theoretical calculation

1. Introduction

Nitrogen trifluoride, NF_3, is one of the five presently known binary N–F compounds [1]. First discovered by Ruff in 1928 [2], its structure, bonding, and molecular properties have been extensively investigated for many years [3], and new information is still emerging [4,5]. At low temperatures, NF_3 reacts only sluggishly, particularly in the absence of reducing metals. The thermodynamically favoured reactions with H_2, CH_4, CO, H_2O, H_2S, and many other compounds are prevented, at ambient temperatures, by kinetic factors. The N–F bonds of NF_3 are however relatively weak (the average value is less than 70 kcal mol^{-1} [6]) and may be dissociated by plasma or thermal techniques. This decomposition is fast, efficient (up to ca. 90–95%), and does not produce solid residues. For these reasons, NF_3 is extensively used in the semiconductor industry to perform etching and cleaning processes [7]. This industrial use has in fact recently increased to such an extent that the adverse environmental impact of NF_3 as a potent greenhouse gas is becoming of concern [8,9].

Despite the great chemical stability of NF_3, the gaseous NF_x^+ ($x = 1$–3) are highly reactive and undergo various ionic processes with, for example, NF_3 itself [10], CH_4 [11,12], H_2O [13–15], H_2S [16], HN_3 [17], $H_2N{-}CN$ [18], CO [19,20], and N_2O [21]. Various ion–molecule reactions involving the neutral NF_3 have been also observed and investigated [22–24]. The interest in this chemistry, that started essentially for fundamental reasons [11,12], has become progressively related to the above-mentioned industrial use of NF_3. In fact, during the etching and cleaning processes, the dissociation of pure or diluted (for example, with helium, argon, or oxygen) NF_3 generates the chemically active fluorine atoms as well as ionic species such as NF_x^+ ($x = 1$–3), N_2F^+, and NO_x^+ ($x = 1, 2$) [25] whose active role is substantiated by experimental [26–28] and theoretical evidence [29,30]. A detailed knowledge of the ion chemistry of NF_3/O_2 and NF_3/N_2 gaseous mixtures is also of interest

* Corresponding author. Tel.: +39 0761 357126; fax: +39 0761 357179.
E-mail address: fgrandi@unitus.it (F. Grandinetti).

1387-3806/$ – see front matter © 2007 Elsevier B.V. All rights reserved.
doi:10.1016/j.ijms.2007.07.011

for the proposed use of O_2- and N_2-based plasmas [31,32] to reduce the atmospheric emissions of NF_3. For example, a recent kinetic modeling of the NF_3 decomposition via dielectric barrier discharge in NF_3/N_2 [33] lists nearly twenty ionic processes involving NF_3 and NF_x^+ ($x = 1$–3). Finally, the chemical inertness of NF_3 toward the major neutral tropospheric oxidants [8] stimulates interest in the conceivable occurrence of ionic processes promoted, for example, by inorganic aerosols or by corona discharges during natural events.

The present mass spectrometric and theoretical study on the positive and negative ion–molecule reactions occurring in NF_3/SO_2 mixtures reveals novel motifs of the gas-phase ion chemistry of NF_3. In particular, few processes involving NF^+ have been observed and discussed in detail, and we report here the efficient activation of the OS–O bond by NF^+ with formation of the atmospherically relevant FNO, FSO, SO^+, and NO^+. We have also observed the formation of FSO_x^+ ($x = 1$, 2) from the efficient oxidative fluorination of SO_x^+ by NF_3. This provides a novel route to the cationic sulfur oxyfluorides, a group of reactive intermediates involved in the corona discharge decomposition of SF_6 [34–36]. We have also observed the formation of FSO_2^- from the reaction between SO_2^- and NF_3, and obtained preliminary insights into the still unexplored gas-phase reactivity of FSO_2^+.

2. Experimental and computational details

The experiments in the positive ionisation mode were performed using a Finnigan ITMS instrument maintained at 333 K. Reagent gases and buffer helium were introduced into the trap at typical pressures of ca. 6.0×10^{-7} and ca. 1.0×10^{-4} Torr (1 Torr = 133 Pa), respectively, empirically set so to maximize the abundance of the signals and measured by a Bayard Alpert ion gauge. The nominal values were corrected for different sensitivity toward different gases,[1] and for a calibration factor which depends on the geometry of the instrument [37]. These pressure domains, while ensuring appreciable signal-to-noise (S/N) ratios, prevent however too much high ion densities into the trap. This avoids space-charge effects which may compromise *m*/*z* ratio assignments or cause problems of mass discrimination. Ion densities are also optimized with respect to ionization times by an Automatic Gain Control [38]. While mass accuracy can be in principle reduced when resonance ejection is used to extend the *m*/*z* ratio beyond the standard highest limit of the commercial ion trap of 650 [38], our investigated mass-to-charge ratios are invariably well below this highest limit. Therefore, even though we have not performed specific determinations of the dynamic range, we may reasonably assume that it is linear for all the experiments performed. Electron ionisation was achieved by an electron beam of 35 eV (average energy). The reaction sequences and the rate constants were determined by selective ion storage of the reactant ions performed by the apex method (superimposition of dc and rf voltages). This avoids the presence of interference ions and allows to maximize the abundance of selected ions so to obtain appreciable S/N ratios. Secondary reactions were also minimized by typical reaction times of less than 40 ms. Linear kinetic plots were invariably obtained for the decay of any selected ion. The scan modes and the methods used for the data processing have been already described previously [37] and will not be repeated here. Assuming the usual uncertainties in measuring absolute pressures with the Bayard Alpert ion gauge, the phenomenological rate constants are the average of two determinations and are expected to be accurate within ±20%. The ions detection range was set between 10 and 300 Th. Collisional-activated dissociation (CAD) experiments were performed by setting the following ITMS parameters: ion storage time: 10–20 ms; q_z value: 0.45; helium buffer gas pressure: 6.5×10^{-4} Torr; tickle voltage: 4000 mV. The resonant excitation frequency was manually adjusted to improve the fragmentation efficiency.

The experiments in the negative ionisation mode were performed using a Finnigan GCQ Polaris mass spectrometer maintained at room temperature. Electron ionisation (EI) and chemical ionisation (CI) were both achieved by an electron beam of 35 eV (average energy) and an ionisation time of 25 ms. The EI and CI experiments were however performed using two different types of ion volumes (source geometry). The EI volume is open but the CI one is closed and with a small hole for leaking ions. This allows higher effective pressures and facilitates CI conditions. A modified inlet system allowed the introduction of gases into the ion source through the transfer-line inlet. Gas pressures were regulated with a needle valve and ranged from 1.0×10^{-6} to 1.0×10^{-5} Torr for reactant gases, and from 1.0×10^{-5} to 5.0×10^{-5} Torr for helium. These values correspond to the pressures read by a Granville-Phillips ion gauge. Due to high-pressure conditions, any obtained spectrum should be in principle regarded as a CI spectrum. The EI/CI notation is however adopted to distinguish the use of the EI or the CI ion volume. Selected ions were isolated by imposition of the ac isolation waveform voltage applied to the end cap electrodes of the ion trap, in combination with the main rf voltage. Ion–molecule reactions were observed at variable storage times of up to 100 ms, obtained by modification of the standard software of the instrument. Difficulties encountered in the calibration of the ion gauge prevent however the measurement of rate constants by the GCQ instrument. The use of standard reactions, including the pseudo-first order decay of CH_4^+ reacting with methane [39], is in fact precluded by the low abundance of the precursor ions invariably obtained in the high pressure domain of the ion source.

NF_3 (Rivoira, >99.99%) and SO_2 (SIAD, 99.99%) were dried by sodium sulfate before using, while He (SIAD, 99.998%) was used without further purification.

The calculations were performed with the GAUSSIAN 03 [40] and MOLPRO 2000.1 [41] sets of programs using the standard internal 6-311+G(2df) basis set [42]. The geometries were optimised at the Becke's three-parameter hybrid functional level of theory, B3LYP [43], where the non-local correlation is provided by the Lee–Yang–Parr expression [44]. The obtained structures were ascertained to be true minima on the B3LYP potential energy surface by calculating their harmonic vibrational frequencies. The unscaled values were also used to

[1] M. Decouzon, J.F. Gal, P.C. Maria, A.S. Tchinianga, private communication.

Table 1
Positive ion–molecule reactions in ionised NF_3/SO_2

Reaction	k_{exp}	$\sum k_{exp}$	k_{coll}[a]	Efficiency[b]	ΔH (kcal mol^{-1})[c]
$NF^+ + SO_2 \rightarrow NO^+ + FSO$	1.2		9.7	0.62	−102.7[d]/−106.1[e]
$NF^+ + SO_2 \rightarrow SO^+ + FNO$	4.6				−48.5
$NF^+ + SO_2 \rightarrow SO_2^+ + NF$	0.2	6.0			2.1
$NF_2^+ + SO_2 \rightarrow$ No reaction					
$NF_3^+ + SO_2 \rightarrow SO_2^+ + NF_3$	4.1	4.1	7.8	0.53	−13.6
$S^+ + NF_3 \rightarrow$ No reaction					
$SO^+ + NF_3 \rightarrow FSO^+ + NF_2$	6.8	6.8	8.3	0.82	−27.3
$SO_2^+ + NF_3 \rightarrow FSO_2^+ + NF_2$	1.7		7.7	0.27	−25.0
$SO_2^+ + NF_3 \rightarrow NF_2^+ + FSO_2$	0.4	2.1			3.4[f]/−0.2[g]
$FSO_2^+ + NF_3 \rightarrow NF_2^+ + F_2SO_2$	5.1	5.1	7.2	0.71	−18.6
$FSO_2^+ + NF_3 \rightarrow NF_2^+ + F_2 + SO_2$					91.8

Rate constants are expressed as 10^{-10} cm^3 molecule^{-1} s^{-1}; uncertainty is within 20%. Despite the presence of buffer helium, it is always difficult to estimate how truly thermal the ions are in an ion trap. The quoted values must be therefore regarded as phenomenological rate constants.

[a] Collisional rate constants have been calculated according to the Parametrized Trajectory Theory (Ref. [56]) taking the polarizability of NF_3 and SO_2 from Ref. [57].

[b] Calculated as the ratio $\sum k_{exp}/k_{coll}$.

[c] Based on the thermochemical data at 298 K listed in Table 2.

[d] Based on the theoretical ΔH_f° of FSO from Ref. [36].

[e] Based on the theoretical ΔH_f° of FSO from Ref. [58].

[f] Based on the theoretical ΔH_f° of FSO_2 from Ref. [36].

[g] Based on the theoretical ΔH_f° of FSO_2 from Ref. [58].

evaluate the zero-point energies and the vibrational contribution to the thermal correction at 298.15 K [45] (both the translational and the rotational contribution were evaluated as (3/2)RT). The total energies of the investigated molecules and ions were subsequently refined by single-point calculations at the restricted coupled cluster level of theory [46–49], including the contribution from single and double substitutions, and an estimate of connected triples. The atomic charges were calculated by natural bond orbital (NBO) analysis [50] of the B3LYP/6-311+G(2df) wave function.

3. Results and discussion

3.1. Reactions between SO_x^+ (x = 1, 2) and NF_3

Fig. 1 shows a typical time-delayed mass spectrum from ionised NF_3/SO_2.

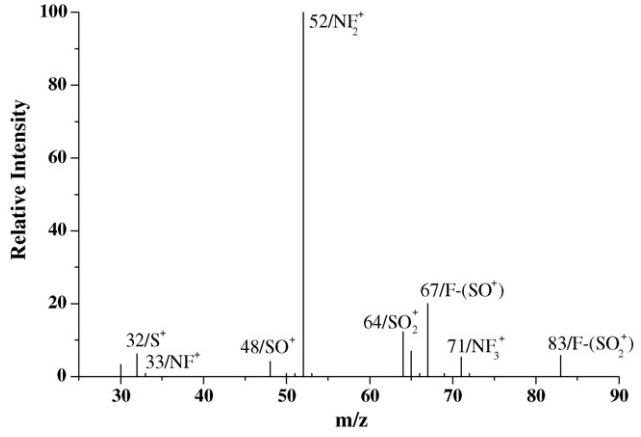

Fig. 1. 35 eV positive mass spectrum of NF_3/SO_2 (reaction time: 100 ms).

Besides the signals from NF_3 (NF^+: $m/z = 33$; NF_2^+: $m/z = 52$; NF_3^+: $m/z = 71$) and SO_2 (S^+: $m/z = 32$; SO^+: $m/z = 48$; SO_2^+: $m/z = 64$), we note in particular the two readily detected peaks at $m/z = 67$ and $m/z = 83$. These ions arise exclusively from the F-abstraction reactions

$$SO^+ + NF_3 \rightarrow F\text{–}(SO)^+ + NF_2 \quad (1)$$

$$SO_2^+ + NF_3 \rightarrow F\text{–}(SO_2)^+ + NF_2 \quad (2)$$

(all the presently observed ion–molecule reactions and their relevant thermochemical data are listed in Tables 1 and 2, respectively. The rate constants are obtained from kinetic plots such as the one reported in Fig. 2).

The results of previous ab initio calculations [34] suggest the nearly exclusive formation of the singlet sulfur–fluorine cations F–S–O$^+$ and F–S(O)–O$^+$. The Gaussian-3 (G3) enthalpy of formation (ΔH_f°) of the singlet F–S–O$^+$ is in fact 164.6 ± 2 kcal mol^{-1}, which is consistent with an experimental estimate of 169.5 ± 1.6 kcal mol^{-1} based on the appearance

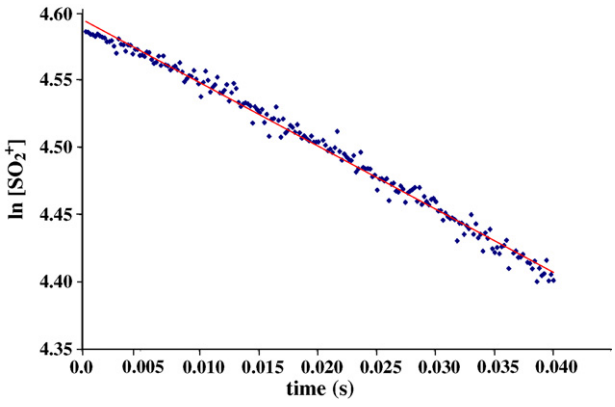

Fig. 2. Time dependence of ln[SO_2^+] for the reaction between SO_2^+ and NF_3.

Table 2
Thermochemical data (ground state, 298 K) of the species involved in the positive ion–molecule reactions in ionised NF_3/SO_2

Neutral	IE (eV)	ΔH_f° (kcal mol^{-1})	Ion	ΔH_f° (kcal mol^{-1})
NF	12.26	59.5	NF^+	342.2[a]
NF_2	11.63	10.1	NF_2^+	278.3[a]
NF_3	12.94	−31.6	NF_3^+	266.8[a]
SO	10.29	1.2	SO^+	238.5[a]
SO_2	12.35	−70.9	SO_2^+	213.9[a]
SF	10.16	3.1	SF^+	237.4[a]
F–SO	9.52[b]	−66.5 ± 3.0[c]	F–SO^+	169.5 ± 1.6[d]
		−69.9 ± 2.0[e]		164.6 ± 2.0[f]
F–SO_2		−92.6 ± 3.0[c]	F–SO_2^+	147.2 ± 1.6[g]
		−96.2 ± 3.0[e]		156.6 ± 2.0[f]
F_2SO_2	13.04	−181.3	$F_2SO_2^+$	119.4[a]
NO	9.26	21.6	NO^+	235.1[a]
F–NO	12.65	−15.7	F–NO^+	276.0[a]
O_2	12.07	0	O_2^+	278.3[a]
O	13.62	59.6	O^+	373.7[a]
F	17.42	19.0	F^+	420.7[a]
S	10.36	66.2	S^+	305.1[a]

Unless stated otherwise, all thermochemical data are taken from Ref. [6].
[a] Obtained as the sum of the ΔH_f° and the IE of the corresponding neutral.
[b] QCISD/6-311G(2df) theoretical estimate from Ref. [52].
[c] G2 "corrected" theoretical estimate from Ref. [36].
[d] Based on the appearance energy from F_2SO_2 of 18.62 ± 0.07 eV quoted in Ref. [51].
[e] CBS-q theoretical estimate from Ref. [58].
[f] G3 theoretical estimate from Ref. [34].
[g] Based on the appearance energy from F_2SO_2 of 15.07 ± 0.07 eV quoted in Ref. [51].

energy (AE) of structurally unknown FSO^+ from F_2SO_2 [51]. Therefore, from Table 2, assuming the formation of this ion, reaction (1) is exothermic by nearly 27 kcal mol^{-1}. The formation of triplet F–S–O^+ and of any singlet or triplet F–O–S^+ is instead substantially endothermic, as their G3 ΔH_f°s range from 230 to 270 kcal mol^{-1} [34]. As for reaction (2), the G3 ΔH_f° of the singlet F–S(O)–O^+ is 156.6 ± 2 kcal mol^{-1} [34], which is only slightly higher than the experimental estimate of 147.2 ± 1.6 kcal mol^{-1} based on the AE of structurally unknown FSO_2^+ from F_2SO_2 [51]. Therefore, assuming the formation of this ion, reaction (2) is exothermic by ca. 20–25 kcal mol^{-1}. The formation of the triplet F–S(O)–O^+ and of any singlet or triplet F–O–SO^+ is instead substantially endothermic, as their G3 ΔH_f°s range from 200 to 260 kcal mol^{-1} [34].

The formation of the singlet F–S–O^+ and F–S(O)–O^+ from reactions (1) and (2) is also consistent with the results of the CAD experiments, which sample in particular the lowest energy decompositions of selected ions [38]. We observed in fact the loss of 19 Th (F atom) from the ion at $m/z = 64$ and the loss of 16 Th (O atom) from the ion at $m/z = 83$. From Table 2, these are indeed the lowest-energy decompositions of the singlet F–S–O^+ and F–S(O)–O^+.

The efficient reactions (1) and (2) are further examples of oxidative fluorinations of gaseous cations by NF_3. Other investigated processes include, for example, the formation of ZnF^+ from Zn^+ [22], of CrF_n^+ ($n = 1$–4) from CrF_{n-1}^+ [24], and of FCO^+ from CO^+ [19]. The mechanistic details of these processes are still poorly understood. We note however from Table 1 that the formation of F–SO_2^+ from reaction (2) is accompanied by a minor but still detectable formation of NF_2^+ and FSO_2. This suggests the intermediacy, along the reaction coordinate, of a $(FSO_2–NF_2)^+$ complex, which dissociates according to two different competitive reaction paths.

The structure and reactivity of the gaseous FSO^+ obtained by air/SF_6 corona discharge have been recently investigated by experimental and theoretical methods [35]. Consistent with our results, structurally diagnostic CAD experiments supported the exclusive formation of the sulfur–fluorine isomer F–S–O^+. In addition, reactivity experiments revealed that this ion is inert toward nucleophiles such as SOF_2, CO, H_2O, N_2, O_2, CO_2, N_2O, SO_2, C_2H_2, and CH_3CN. The only observed reaction was the charge transfer from C_6H_6, whose IE of 9.24 eV is indeed lower than the theoretically predicted value of F–SO, 9.52 eV [52]. In the present study, we found that F–S–O^+ is also unreactive with NF_3. We observed also that F–SO_2^+ is unreactive with SO_2 but undergoes the efficient fluoride abstraction from NF_3. From Table 1, the driving force of this process is the formation of the highly stable F_2SO_2.

3.2. Reactions between NF_x^+ (x = 1–3) and SO_2

NF_2^+ is unreactive toward SO_2, and NF_3^+ undergoes exclusively the efficient exothermic charge transfer. On the other hand, NF^+ forms two abundant ionic products, namely NO^+ and SO^+, and a minor amount of SO_2^+. The formation reactions of NO^+ and SO^+ are exothermic and efficient and provide the first example of molecular activation by NF^+. The only previously observed process is in fact the formation of NF_2^+ by reaction with NF_3 [17]. The formal F^+ transfer between NF^+ and CO has been also theoretically investigated [53]. To explain the somewhat surprising reaction between NF^+ and SO_2, we explored the involved potential energy surface at the B3LYP and coupled cluster level of theory. The relevant results are summarized in Figs. 3 and 4.

NF^+ has a doublet ground state ($^2\Pi$) [54] and its formally empty p orbital may in principle interact with both the oxygen and the sulfur atom of SO_2. We have in fact located two distinct NF^+–(SO_2) energy minima, whose predicted structures are however quite different. The complex **1** located by exploring the ligation of NF^+ to the O atom of SO_2 is indeed an

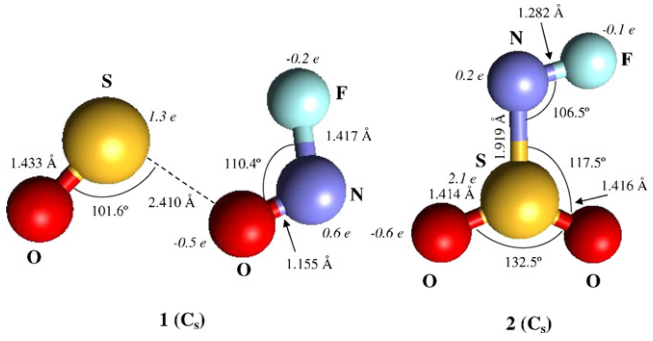

Fig. 3. B3LYP/6-311+G(2df) optimised geometries and NBO atomic charges (italics) of the NF^+–(SO_2) isomers.

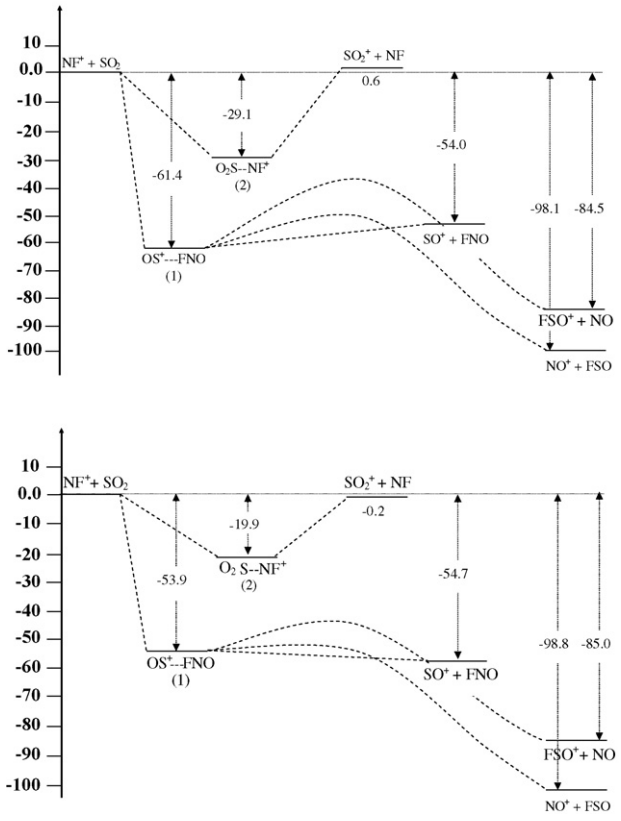

Fig. 4. CCSD(T)/6-311+G(2df)//B3LYP/6-311+G(2df) relative enthalpies (top) and free energies at 298.15 K of the species involved in the reaction between NF^+ and SO_2.

ion–dipole complex between SO^+ and FNO. The S–O distance is as long as 2.4 Å and the two constituent moieties are essentially unperturbed SO^+ and FNO. In addition, according to the large difference between the IE of SO and FNO (see Table 2), the NBO calculations predict a total charge of nearly +1 e on the SO group. From Fig. 3, the formation of **1** is exothermic and exoergic by ca. 60 and ca. 54 kcal mol^{-1}, respectively, and its dissociation into SO^+ and FNO is endothermic by only 7 kcal mol^{-1}, and essentially ergoneutral. This explains the efficient formation (ca. 50%) of SO^+ from the reaction between NF^+ and SO_2. We note also that isomer **1** has two additional exothermic and exoergic exit channels, namely $NO^+ + FSO$ and $FSO^+ + NO$. However, only the former process is experimentally observed with an overall efficiency of nearly 12%. This suggests that the involved activation barrier is comparable with the (barrier-free) dissociation of **1** into SO^+ and FNO.

The reaction between NF^+ and SO_2 produces also minor amounts of SO_2^+. This slightly endothermic but slightly exoergic charge transfer (see Fig. 3) is however not compatible with the formation of isomer **1**. We rather suggest the intermediacy of the sulfur-coordinated isomer **2** located by approaching the empty orbital of NF^+ to the sulfur atom of SO_2. With respect to the S–O distance of isomer **1**, the N–S distance is shorter, and the SO_2 moiety is appreciably perturbed with respect to the free molecule (S–O: 1.443 Å; O–S–O: 118.7°). The complexation enthalpy and free energy are also relatively large and predicted as ca. 29 and ca. 20 kcal mol^{-1}, respectively. The quite similar IEs of NF and SO_2 (see Table 2) suggest also that isomer **2** should feature a significant charge transfer from SO_2 to NF^+. Consistently, the NBO calculations predict a positive charge of the NF moiety of less than 0.2 e. From Fig. 3, the back dissociation of isomer **2** into NF^+ and SO_2 and its dissociation into SO_2^+ and NF involve comparable enthalpy and free energy changes. This explains the low measured efficiency (ca. 2%) of the charge transfer between NF^+ and SO_2.

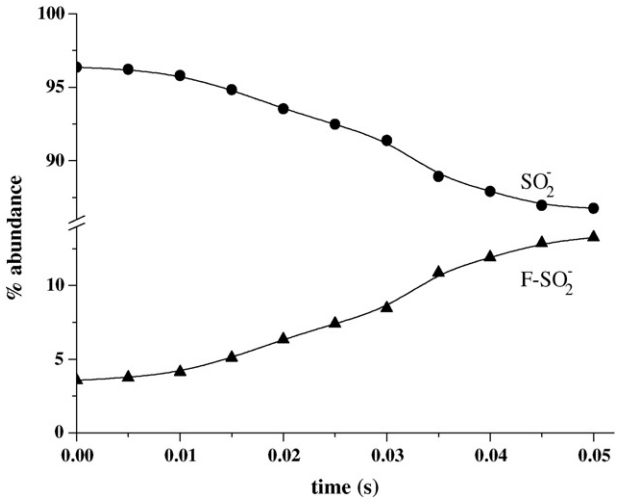

Fig. 5. Time dependence of the percentage abundances of SO_2^- and $F{-}SO_2^-$ for the reaction between SO_2^- and NF_3.

3.3. Negative ion–molecule reactions

Under both EI and CI conditions, the only negative ion–molecule reaction observed in ionised NF_3/SO_2 is the F-atom abstraction

$$SO_2^- + NF_3 \rightarrow F{-}SO_2^- + NF_2 \quad (3)$$

The time-dependence of the intensities of the reactant and product ions is shown in Fig. 5.

Sulfur oxyfluoride anions such as SOF_4^-, SOF_5^-, SO_2F^-, and $SO_2F_2^-$ are formed in SF_6/H_2O negative corona discharge, and their structure, bonding, and thermochemistry have been investigated by experimental and theoretical methods [36]. In particular, mass spectrometric experiments and G3 calculations [55] indicate that the gaseous $F{-}SO_2^-$ has a sulfur–fluorine connectivity and a non-planar structure of C_s symmetry. From the measured fluoride affinity of SO_2, 54 ± 2 kcal mol^{-1}, the ΔH_f° of $F{-}SO_2^-$ is obtained as -184 ± 2 kcal mol^{-1}. Reaction (3) is therefore exothermic by 46 kcal mol^{-1}, and it is the first observed fluorination of a gaseous anion by NF_3. This suggests a novel still unexplored strategy for the preparation of gaseous fluorinated anionic species.

4. Concluding remarks

Nitrogen trifluoride is extensively used in the electronic industry to perform etching and cleaning processes. Once released in the atmosphere, it is inert toward the major tropospheric oxidants, and it is therefore of interest to investigate

its conceivable participation in ionic processes. Our experimental and theoretical study reveals that, in the presence of SO_2, ionised NF_3 undergoes the efficient formation of ionic and neutral species such as NO^+, SO^+, FNO, and FSO, which may be indeed of atmospheric relevance. Ionized SO_2 also reacts with NF_3 giving FSO^+ and $FSO_2{}^+$. From a fundamental point of view, we have reported here the first case of chemical activation by NF^+, and the possible use of NF_3 as a fluorinating agent of gaseous anionic species.

Acknowledgements

The authors thank the Università degli Studi di Torino, the Università della Tuscia, and the Italian Ministero dell' Università e della Ricerca (MiUR) for financial support through the "Cofinanziamento di Programmi di Ricerca di Rilevante Interesse Nazionale".

References

[1] T.M. Klapötke, J. Fluorine Chem. 127 (2006) 679, and references therein.
[2] O. Ruff, J. Fischer, F. Luft, Z. Anorg. Allg. Chem. 172 (1928) 417.
[3] C.J. Hoffman, R.G. Neville, Chem. Rev. 62 (1962) 1.
[4] T.D. Kolomiitsova, D.N. Shchepkin, K.G. Tokhadze, W.A. Herrebout, B.J. van der Veken, J. Chem. Phys. 121 (2004) 1504.
[5] G. Cazzoli, C. Puzzarini, J. Mol. Spectrosc. 239 (2006) 59.
[6] Unless stated otherwise, all thermochemical data are taken from: P.J. Linstrom, W.G. Mallard (Eds.), NIST Chemistry Webbook, NIST Standard Reference Database Number 69, June 2005 Release, National Institute of Standard and Technology, Gaithersburg, MD, 20899 (http://webbook.nist.gov).
[7] A. Tasaka, J. Fluorine Chem. 128 (2007) 296, and references therein.
[8] L.T. Molina, P.J. Wooldridge, M.J. Molina, Geophys. Res. Lett. 22 (1995) 1873.
[9] J.I. Robson, L.K. Gohar, M.D. Hurley, K.P. Shine, T.J. Wallington, Geophys. Res. Lett. 33 (2006) L10817.
[10] K. Hiraoka, M. Nasu, S. Fujimaki, S. Yamabe, J. Phys. Chem. 99 (1995) 15822.
[11] J.J. Fisher, T.B. McMahon, J. Am. Chem. Soc. 110 (1988) 7599.
[12] F. Grandinetti, J. Hrušàk, D. Schröder, S. Karrass, H. Schwarz, J. Am. Chem. Soc. 114 (1992) 2806.
[13] F. Cacace, F. Grandinetti, F. Pepi, Angew. Chem. Int. Ed. Engl. 33 (1994) 123.
[14] M. Aschi, F. Cacace, F. Grandinetti, F. Pepi, J. Phys. Chem. 98 (1994) 2713.
[15] M. Aschi, F. Grandinetti, F. Pepi, Int. J. Mass Spectrom. Ion Process. 130 (1994) 117.
[16] F. Grandinetti, A. Ricci, Chem. Phys. Lett. 253 (1996) 189.
[17] F. Cacace, F. Grandinetti, F. Pepi, Inorg. Chem. 34 (1995) 1325.
[18] F. Cacace, F. Grandinetti, F. Pepi, J. Chem. Soc. Chem. Commun. (1994) 2173.
[19] F. Grandinetti, F. Pepi, A. Ricci, Chem. Eur. J. 2 (1996) 495.
[20] M. Aschi, F. Grandinetti, V. Vinciguerra, Chem. Eur. J. 4 (1998) 2366.
[21] F. Cacace, F. Grandinetti, F. Pepi, J. Phys. Chem. 98 (1994) 8009.
[22] J.E. Bartmess, J.G. Kester, Inorg. Chem. 23 (1984) 1877.
[23] T.M. Miller, J.F. Friedman, A.E.S. Miller, J.F. Paulson, J. Phys. Chem. 98 (1994) 6144.
[24] U. Mazurek, D. Schröder, H. Schwarz, Collect. Czech. Chem. Commun. 63 (1998) 1498.
[25] See, for example: H.-P. Hsueh, R.J. McGrath, B. Ji, B.S. Felker, J.G. Langan, E.J. Karvacki, J. Vac. Sci. Technol. B 19 (2001) 1346.
[26] T.W. Little, F.S. Ohuchi, Surf. Sci. 445 (2000) 235.
[27] J.G. Langan, S.E. Beck, B.S. Felker, S.W. Rynders, J. Appl. Phys. 79 (1996) 3886.
[28] M. Konuma, E. Bauser, J. Appl. Phys. 74 (1993) 62.
[29] A. Endou, T.W. Little, A. Yamada, K. Teraishi, M. Kubo, S.S.C. Ammal, A. Miyamoto, M. Kitajima, F.S. Ohuchi, Surf. Sci. 445 (2000) 243.
[30] A. Jenichen, J. Phys. Chem. 100 (1996) 9820.
[31] Y.F. Wang, L.C. Wang, M.L. Shin, C.H. Tsai, Chemosphere 57 (2004) 1157.
[32] J.S. Chang, K.G. Kostov, K. Urashima, T. Yomamoto, Y. Okayasu, T. Kato, T. Iwaizumi, K. Yoshimura, IEEE Trans. Ind. Appl. 36 (2000) 1251.
[33] H.L. Chen, H.M. Lee, M.B. Chang, Plasma Process. Polym. 3 (2006) 682.
[34] P. Antoniotti, P. Facchini, F. Grandinetti, Chem. Phys. Lett. 372 (2003) 455.
[35] F. Pepi, A. Ricci, M. Di Stefano, M. Rosi, Chem. Phys. Lett. 381 (2003) 168.
[36] S.T. Arnold, T.M. Miller, A.A. Viggiano, J. Phys. Chem. A 106 (2002) 9900.
[37] L. Operti, M. Splendore, G.A. Vaglio, A.M. Franklin, J.F.J. Todd, Int. J. Mass Spectrom. Ion Process. 136 (1994) 25.
[38] R.E. March, J.F.J. Todd, Practical Aspects of Ion Trap Mass Spectrometry, vol. I, CRC Press, Boca Raton, 1995.
[39] M.T. Bowers (Ed.), Gas Phase Ion Chemistry, vol. 1, Academic Press, New York, 1979.
[40] M.J. Frish, G.W. Trucks, H.B. Schlegel, G.E. Scuseria, M.A. Robb, J.R. Cheeseman, V.G. Zakrzevski, J.A. Montgomery Jr., T. Vreven, K.N. Kudin, J.C. Burant, J.M. Millam, S.S. Iyengar, J. Tomasi, V. Barone, B. Mennucci, M. Cossi, G. Scalmani, N. Rega, G.A. Petersson, H. Nakatsuji, M. Hada, M. Ehara, K. Toyota, R. Fukuda, J. Hasegawa, M. Hishida, T. Nakajima, Y. Honda, O. Kitao, H. Nakai, M. Klene, X. Li, J.E. Knox, H.P. Hratchian, J.B. Cross, C. Adamo, J. Jaramillo, R. Gomperts, R.E. Stratman, O. Yazyev, A.J. Austin, R. Cammi, C. Pomelli, J.W. Ochterski, P.Y. Ayala, K. Morokuma, G.A. Voth, P. Salvador, J.J. Dannenberg, V.G. Zakrzewski, S. Dapprich, A.D. Daniels, M.C. Strain, O. Farkas, D.K. Malick, A.D. Rabuck, K. Raghavachari, J.B. Foresman, J.V. Ortiz, Q. Cui, A.G. Baboul, S. Clifford, J. Cioslowski, B.B. Stefanov, G. Liu, A. Liashenko, P. Piskorz, I. Komaromi, R.L. Martin, D.J. Fox, T. Keith, M.A. Al-Laham, C.Y. Peng, A. Nanayakkara, M. Challacombe, P.M.W. Gill, B.G. Johnson, W. Chen, M.W. Wong, C. Gonzalez, J.A. Pople, GAUSSIAN 03, Revision C.02, Gaussian, Inc., Wallingford, CT, 2004.
[41] MOLPRO is a package of ab initio programs written by H.-J. Werner and P.J. Knowles, with contributions from R.D. Amos, A. Bernhadsson, A. Berning, P. Celani, D.L. Cooper, M.J.O. Deegan, A.J. Dobbyn, F. Eckert, C. Hampel, G. Hetzer, T. Korona, R. Lindh, A.W. Lloyd, S.J. McNicholas, F.R. Manby, W. Meyer, M.E. Mura, A. Nicklass, P. Palmieri, R. Pitzer, G. Rauhut, M. Schatz, H. Stoll, A.J. Stone, R. Tarroni, and T. Thorsteinsson.
[42] W.J. Hehre, L. Radom, P.v.R. Schleyer, J.A. Pople, Ab initio Molecular Orbital Theory, Wiley, New York, 1986.
[43] P.J. Stephens, F.J. Devlin, C.F. Chabalowski, M.J. Frish, J. Phys. Chem. 98 (1994) 11623.
[44] C. Lee, W. Yang, R.G. Parr, Phys. Rev. B 37 (1988) 785.
[45] D.A. Mc Quarry, Statistical Mechanics, Harper&Row, New York, 1973.
[46] K. Raghavachari, G.W. Trucks, J.A. Pople, M. Head-Gordon, Chem. Phys. Lett. 157 (1989) 479.
[47] C. Hampel, K. Peterson, H.-J. Werner, Chem. Phys. Lett. 190 (1992) 1.
[48] P.J. Knowles, C. Hampel, H.-J. Werner, J. Chem. Phys. 99 (1993) 5219.
[49] J.D. Watts, J. Gauss, R.J. Bartlett, J. Chem. Phys. 98 (1993) 8718.
[50] E.D. Glendening, A.E. Reed, J.E. Carpenter, F. Weinhold, NBO, Version 3.1 (See also: A.E. Reed, L.A. Curtiss, F. Weinhold, Chem. Rev. 88 (1988) 899).
[51] M. Miletić, O. Nešković, M. Veljković, K.F. Zmbov, Rapid Commun. Mass Spectrom. 10 (1996) 1961.
[52] L.A. Muñoz, B.R. Weiner, Y. Ishikawa, J. Mol. Struct. (Theochem.) 388 (1996) 1.
[53] M. Aschi, F. Grandinetti, Int. J. Mass Spectrom. 201 (2000) 151.
[54] J. Czernek, O. Živny, Chem. Phys. 303 (2004) 137.
[55] K.C. Lobring, C.E. Check, L.S. Sunderlin, Int. J. Mass Spectrom. 222 (2003) 221.
[56] T. Su, W.J. Chesnavich, J. Chem. Phys. 76 (1982) 5183.
[57] R.D. Lide (Ed.), CRC Handbook of Chemistry and Physics, 73rd ed., CRC Press, Boca Raton, FL, 1992.
[58] M.P. Badenes, M.E. Tucceri, C.J. Cobos, Z. Phys. Chem. 214 (2000) 1193.